Peer-reviewed version available at Forests 2019, 10, 959; doi:10.3390/f10110959

Article

Detection and Microscopy of *Alnus glutinosa* Pollen Fluorescence Peculiarities

Ingrida Šaulienė[1]*, Laura Šukienė[1], Gintautas Daunys[1], Gediminas Valiulis[1], Alfredas Lankauskas[1], Inese Kokina[2], Vjačeslavs Gerbreders[2], and Inese Gavarāne[2]

[1] Institute of Regional Development, Šiauliai University, Šiauliai, 76351 Lithuania; laura.sukiene@su.lt (L.Š.); gintautas.daunys@su.lt (G.D.); gediminas.valiulis@su.lt (G.V.); alfredas.lankauskas@su.lt (A.L.)

[2] Institute of Life Science and Technology, Daugavpils University, Daugavpils, LV5401 inese.kokina@du.lv (I.K.); vjaceslavs.gerbreders@du.lv (V.G.); inese.gavarane@du.lv (I.G.)

* Correspondence: ingrida.sauliene@su.lt; Tel.: +370-41-595886 (I. Š.)

Abstract: *Alnus glutinosa* is important woody plant in Lithuanian forest ecosystems. Knowledge of fluorescence properties of black alder pollen is necessary for scientific and practical purposes. By the results of the study we aimed to evaluate possibilities of identifying *Alnus glutinosa* pollen fluorescence properties by modeling ozone effect and applying two different fluorescence-based devices. To implement experiments, black alder pollen was collected in a typical habitat during the annual flowering period in 2018-2019. There were three groups of experimental variants, which differed in the duration of exposure to ozone, conditions of pollen storage before the start of the experiment, and the experiment start time. Data for pollen fluorescence analysis were collected using two methods. The microscopy method was used in order to evaluate the possibility of employing image analysis systems for investigation of pollen fluorescence. The second data collection method is related to the automatic device identifying pollen in real time, which uses the fluorescence method in the pollen recognition process. Data were assessed employing image analysis and principal component analysis (PCA) methods. Digital images of ozone-exposed pollen observed under the fluorescence microscope showed the change of the dominant green colour towards the blue spectrum. Meanwhile, the automatic detector detects more pollen whose fluorescence is at the blue light spectrum. It must be noted that assessing pollen fluorescence several months after exposure to ozone, no effect of ozone on fluorescence remains.

Keywords: allergenic pollen; ozone, automatic real-time device; image analysis; principal component analysis

1. Introduction

Pollen, like any airborne particle of biological origin, can be identified using fluorescence examination methods. Application of possibilities of these methods in the bioparticle identification process promotes designing and development of laser-fluorescence-based devices for recognising airborne pollen in real time [1–3]. The topics of pollen fluorescence have been the focus of scientists for many years and this issue is constantly readdressed. Identification of fossil pollen and spores in geological samples and the possibility of dating contaminated sediments became a strong impetus for gathering knowledge of pollen fluorescence. Fluorescence-microscopical techniques and the physical and chemical nature of pollen walls expanded the possibilities of palynological research. Upon performance of first laboratory tests, it was identified that pollen fluoresced under ultraviolet light [4], while fresh and subfossil pollen grains and spores showed various fluorescence colours, depending on type or species [5]. Studies on pollen in geological samples confirm that the exine of a pollen grain is naturally autofluorescent and the strength of the fluorescence varies with exine thickness [6]. Fluorescence microscopy turned into a tool for studying different pollen type

morphology, while acquired knowledge became valuable in analysing not only fossil biological origin particles but also airborne particles [7–11].

Studies on fluorescence of airborne particles (pollen and spores) were encouraged not that much by the aspiration to acquired additional knowledge of particle morphology, but by assessment of practical possibilities of applying the method itself. A new stimulus of employing the fluorescence method is a growing demand for devices capable of automatic identification of the airborne pollen and spores. Fluorescence microscopy has been used to develop 3D volumetric imaging technology [7], in particular designing the online pollen monitoring system. At present, microscopy techniques for identification of pollen and spores still prevail worldwide [12]. These methods have become traditional in aerobiology [13–14], requiring that specialists should identify each particle present in air samples under the microscope. For more than fifteen years there have been attempts to develop semi-automatic [1,15] or automatic [7,10,16] pollen identification systems, in which the use of the fluorescence method for identification of air origin particles occupies an important place. However, to date, the results of collected data, gained by automatic real-time devices, differ [10–11,17–18], and these differences may be determined not only by peculiarities of devices but also by conditions of the environment affecting identified pollen [19–22]. This fact is confirmed by scientific studies that are targeted at the long-distance pollen transport analysis [23–29]. It is assumed that pollen suspending in the air are affected by environmental conditions (air temperature, humidity, radiation, chemical compounds) and the effect may change pollen fluorescence results (intensity, colour, etc.). Laboratory tests showed that pollen had chemosensitivity to ozone and ozone could directly oxidize the constituents of the pollen wall [30–31], although the number of pollen grains produced per inflorescence was unaffected by ozone [32]. There is scientific evidence that ozone alters the allergen content in the pollen [33–35], reduces or destroys viability of the pollen [36–38], and changes fluorescence properties of fluorescent substances present in pollen [8,30–31]. Studies on pollen fluorescence properties are conducted employing various devices ranging from the microscope to devices enabling automatic identification. Their application in routinely performed monitoring of airborne pollen requires specific knowledge.

By the results of the study we aimed to evaluate possibilities of identifying *Alnus glutinosa* pollen fluorescence properties by modeling ozone effect and applying two different fluorescence-based devices.

2. Materials and Methods

2.1. Pollen samples

Alnus glutinosa ((L.) Gaertn.) is important woody plant in Lithuanian forest ecosystems. It is the fourth most abundant tree in Lithuanian forests and its occurrence in Lithuania's forest stand is around 8.5% [39]. Black alder is one of the earliest flowering plants producing abundant content of allergenic pollen [40].

Catkins for the experiments were collected in the forest, in the typical habitat of *Alnus glutinosa* during the annual flowering period. Catkins were collected from the same plant in 2018 in the beginning of April; and in 2019, in the end of March. Weather conditions (data taken from Lithuanian hydrometeorological service Šiauliai weather station) in 2018 and in 2019 from January until collection of catkins were different (Table 1). The beginning of 2019 was colder and the average air temperature in February and March was higher than in 2018.

Table 1. Meteorological conditions in January-March of 2018-2019

Years	Average monthly air temperature (°C)			Total precipitation per month (mm)		
	January	February	March	January	February	March
2018	-1,6	-6,6	-2,1	51,1	15,8	12,8
2019	-4,0	1,3	3,1	54,0	38,4	31,8

In 2018, catkins were kept in a thermostatic convection oven in the laboratory for three days at 40°C; and in 2019, at 30°C. The procedure of pollen separation from catkins was performed according

Peer-reviewed version available at Forests 2019, 10, 959; doi:10.3390/f10110959

to Šaulienė et al. [11]. Until the start of the experiment in 2018, clean, impurity-free pollen was stored in the refrigerator at temperature of 5±1°C and relative humidity of 57±10%; and in 2019, was kept indoors at 25±5°C and 45±10%, respectively.

2.2. Pollen exposures to O_3

The experiments were carried out in laboratory conditions using ozone generator operating on the high voltage discharge principle. Ozone is generated in a sealed plastic box containing a system of insulators and electrodes. The applied high voltage (approx. 25 kV) to the electrodes creates ionisation current that passes through an air gap and gives high energy to electrons to break the oxygen molecule, allowing the formation of a 3-atom oxygen molecule – ozone (Fig 1).

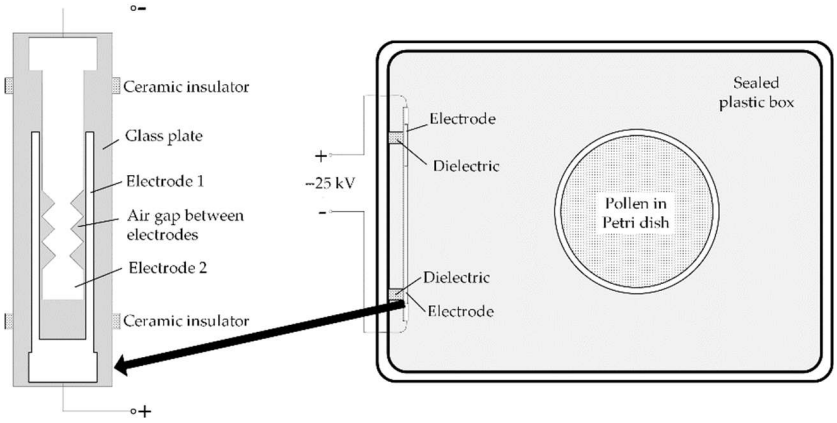

Figure 1. Pollen sample exposure to O_3 experimental set-up and high voltage electrical discharge system configuration

5 mg of *Alnus glutinosa* pollen were dispersed in two 100-mm-diameter Petri dishes and placed in a generator box (Fig 1). The first sample was kept in a running generator for 3 hours per day; and the second sample, for 5 hours. The experiment was run for 5 days of the week. In total, the first sample was exposed to ozone for 15 hours; and the second, for 25 hours. The average measured ozone concentration was 5.83 ppm. The measurements were performed using GV-100 gas sampling pump with colorimetric tubes GASTEC Ozone 18L and GASTEC Ozone 18M.

Groups of experimental variants of pollen, formed this way (Table 2), differed in the duration of exposure to ozone, pollen storage conditions until the start of the experiment, and the time of their use in the experiment; i.e., from collection of pollen from catkins until the start of the experiment.

Table 2. Groups of experimental variants of pollen

Name of the group of experimental variant	Abbreviation	Time of exposure to ozone, hours	Storage	Duration of storage until the start of the experiment, months
Control	CS_1	0	In the refrigerator	5
	C_1	0	Indoors	1
	C_2	0	Indoors	5
3-hour exposure	3h_1	3	Indoors	1
	3h_2	3	Indoors	5
5-hour exposure	5h_1	5	Indoors	1
	5h_2	5	Indoors	5

2.3.1. Fluorescence by microscope

Within 5-6 days after exposure to ozone, pollen was prepared for microscopy. Pollen samples were prepared for work with the fluorescence microscope having scattered pollen on slides. They were embedded into a solution of polyvinylalcohol (Gelvatol) [41,42]. Pollen was photographed with Nikon ECLIPSE 80I fluorescence microscope, using x400 magnification. Samples were paced under UV light. To obtain the fluorescence image, three ND (4, 8, 16) filters were used. Pollen images was digitized at random, but not less than 200 pollen per one type (pollen not affected by ozone/ozone-exposed pollen) sample. Collected digital pollen fluorescence images were analysed using image analysis techniques (see 2.5.1. Image analysis).

2.3.2. Fluorescence by automatic pollen recognition device

The study employed the device Rapid-E, which has capabilities allowing real-time detection, counting and classification of airborne pollen. Identifying airborne particles of biological origin, the device uses the fluorescence method. Fluorescence of particles is excited using the UV laser (320 nm light) [3]. Ozone-exposed black alder pollen and those not affected by ozone was blown into the device using the method described by Šaulienė et al. [11]. The experiment was carried out with *Alnus glutinosa* pollen whose average size was less than 30 μm [43]. For pollen recognition, the device was set in the pollen mode when the range of identified particles was 5-100 μm. Not less than 10000 fluorescent particles were analysed per one type (not exposed to ozone/ozone-exposed pollen) sample.

2.5. Data analysis

2.5.1. Image analysis

The RGB image digitized with the fluorescence microscope contained several or a dozen of pollen. In such cases, it is necessary to find and group pixels belonging to fluorescent pollen and count the statistics of obtained pixels. To achieve this, the following steps were made: image binarization, blob detection, morphological blob correction, turning blobs into masks, pixel selection by masks, conversion of pixel RGB values into HSV space, calculation of statistics in HSV space for each pollen. The actions were implemented in Python programming language using modules matplotlib.image, scipy.ndimage.morphology, scikit-image.

Image binarization requires a threshold value to distinguish the pollen from the background. The threshold value was manually selected for each photo searching for the best option. Blobs were found using the Difference of Gaussian (DoG) method implemented in the scikit-image module. To avoid erroneously detected small areas of the image, the morphological operation erosion was applied. Having applied dilation after erosion, pollen areas are restored to the original area. The obtained blobs served as masks in order to select pixels of individual pollen. Conversion of pixels into HSV space allows to perform averaging of hue values and to obtain a generalized value for describing the fluorescence hue of the pollen. The hue value is expressed in the interval (value in the interval 0 – 1).

2.5.2. Principal component analysis

In the previous research [11], detection of pollen by fluorescence spectrum was performed employing artificial neural networks ANN. However, neural networks prevent from finding out why one or another decision was made. Therefore, although neural networks are widely used today and often yield good recognition results, they can generate many errors if unfavourable conditions are formed. For this reason, in this study, the fluorescence spectrum analysis was performed applying the principal component analysis method (PCA).

Applying PCA method, the correlated variables (in this case, fluorescence amplitudes of certain captured wavelengths of light) are replaced by their linear combinations that are uncorrelated with each other. Besides, these components are ranked according to the average power falling to them. PCA method particularly serves the purpose when the highest power is borne only by a small share of

Peer-reviewed version available at Forests 2019, 10, 959; doi:10.3390/f10110959

components. In this case, the first component used to receive from 65% to 85% of the total power and the first five components, about 95% of the power.

Because of the variety of particles dispersion in the air, the excited laser of Rapid-E device often illuminates other particles than pollen too. Therefore, it is important to filter obtained data, leaving only the pollen spectra for further analysis. Pollen spectra compared to those of various artefacts are wide (the radiation power is distributed in the entire range of visible light rather than a narrow band). Therefore, the first step is to reject fluorescence events where only narrow range light is radiated. To implement this step, the maximum value of the spectrum of one fluorescence event was taken and its ratio with the sum of values of all components of the spectrum was calculated. The obtained ratio must not exceed the experimentally selected threshold value.

The remaining data were subjected to PCA analysis. To perform it, the Python programming language and the scikit-learn module were used. Once the principal components were obtained, fluorescence spectra emission by them was performed, this way obtaining emission coefficients.

The success of method selection was confirmed by its repetition with the data of different samples when the results would replicate well.

3. Results

3. 1. Recognition of ozone effect on pollen under fluorescence microscope

Digitized images of *Alnus glutinosa* pollen fluorescence were analysed in order to evaluate whether high concentrations of ozone and duration of exposure could substantially alter fluorescence peculiarities. The results of the microscope used in this study highlighted inequalities of pollen properties in individual groups of experimental variants. Figure 2 demonstrates several cases illustrating fluorescence variations in groups.

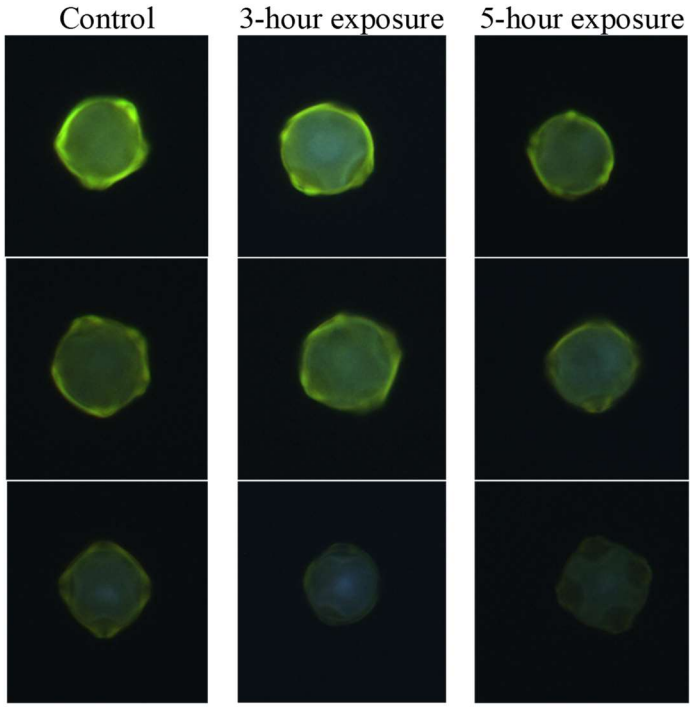

Figure 2. *Alnus glutinosa* pollen image under the fluorescence microscope (400x). The columns show examples of images captured in photos in each of the experimental variant groups.

The given examples show that walls of pollen that are not affected by ozone fluoresce more intensively than of the walls of ozone-exposed pollen. The strength of the fluorescence signal also depends on the duration of ozone exposure. Pollen fluorescence images demonstrated that longer ozone exposure time weakened the fluorescence signal of pollen walls. This statement is verified by

the results given in the column called 5-hour exposure. Comparison of experimental variant groups with each other shows that the fluorescence signal of pollen that was exposed to ozone for the longest time is most altered. Systematized results given in Figure 3 demonstrate shift of the change.

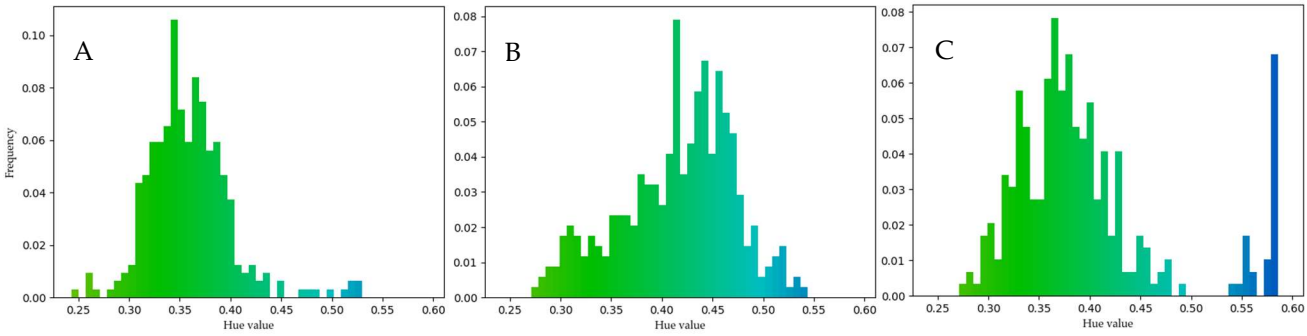

Figure 3. Fluorescence colour dispersion chart of digital images of *Alnus glutinosa* pollen experimental variant groups by hue values: A – control, B – 3-hour exposure, C – 5-hour exposure. The x-axis represents hue values and the y-axis represents the number of cases.

Digital images of fluorescent pollen captured under the microscope were analysed decomposing RGB components. The tendency in the dispersion chart of the control group emerges that by hue values, about 80% of digital image results of pollen not affected by ozone concentrate at the green spectral band. Compared to the control group, the fluorescence results of ozone-exposed pollen differ. Fig. 3B shows shift of results towards the blue portion of the spectrum. This trend is particularly pronounced in the group of experimental variants where pollen was exposed to ozone for 3 hours per day. About 60% of cases cover the portion of the colour spectrum from 0.42 to 0.48. In the case of 3-hour exposure, data scattering is greater than in the case of 5-hour exposure. Here, most results of pollen fluorescence digital images concentrate at the green portion of the spectrum (0.33-0.43 hue values). To sum up, the assumption is formed that the fluorescence microscope used in the study showed slight changes in fluorescence of those pollen that were exposed to ozone for 3 hours.

3.2. Possibilities of the automatic particle detector, assessing ozone effect on pollen

Unlike the image analysis under the fluorescence microscope, the automatic particle detector allows evaluation of the fluorescence spectrum of airborne particles in real time, this way separating biological origin particles from the overall aerosol flow. Because usually the data array while capturing pollen by the automatic particle detector is large, the fluorescence spectrum analysis was performed applying PCA method. In PCA results, it is important to properly evaluate principal components. Figure 4 shows 15 principal (in total, 32) PCA components of the conducted study.

The largest fluorescence amplitude of PCA component 1 includes wavelength from 400 to 550 nm, when the peak is at 450 nm. The peak of PCA component 2, expressed at 350 nm of fluorescence spectrum, is one of the few peaks of PCA components located in short wavelength. Meanwhile, PCA component 4 has several peaks located in the range of different wavelength. The first five PCA components receive about 95% of power. All combined PCA components form the fluorescence spectrum of pollen analysed. Combining all components, a more accurate image of the fluorescence spectrum is formed.

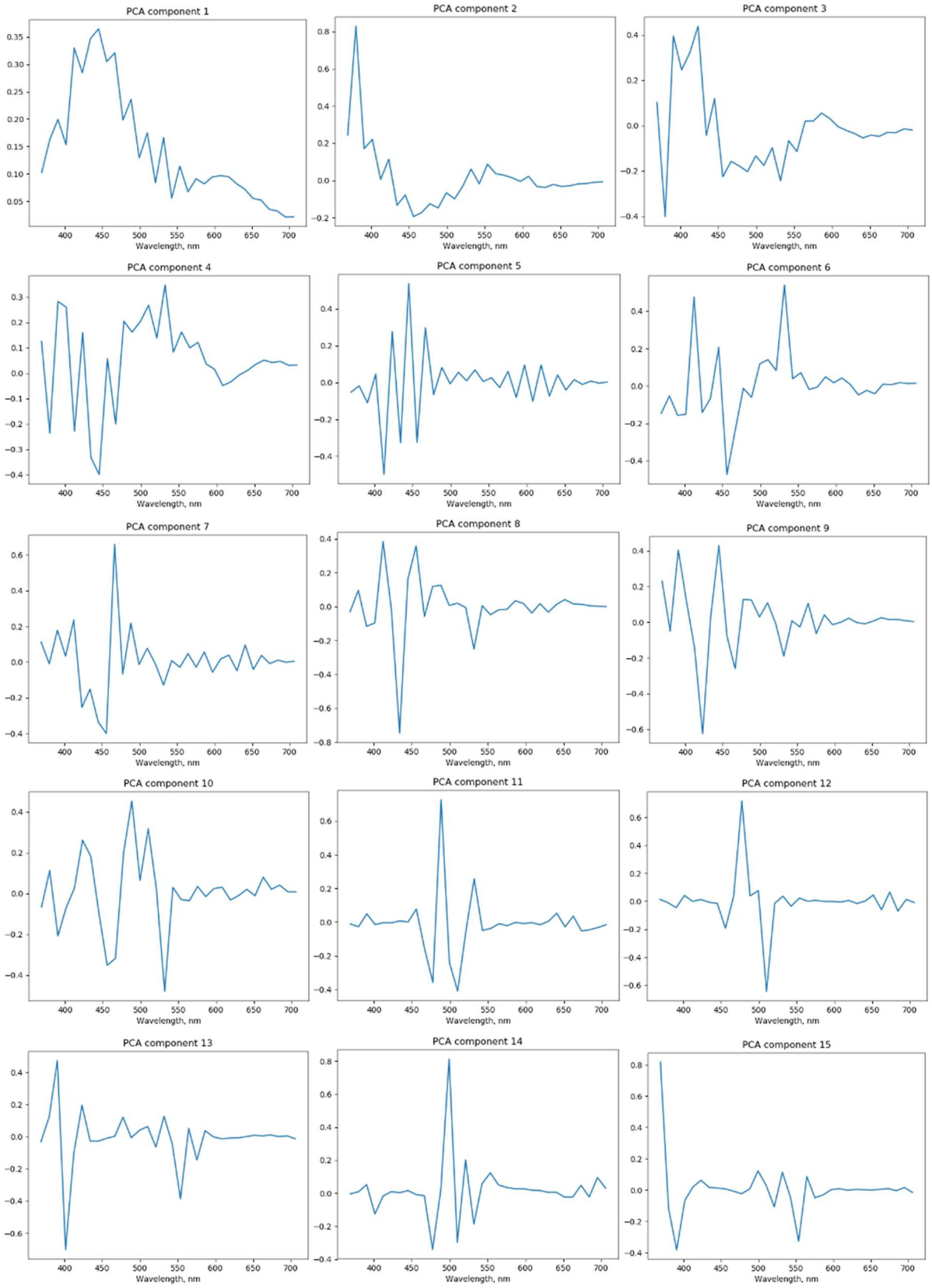

Figure 4. PCA component variety, 15 principal components

However, component 1 is principal and allows to evaluate the shape of the spectrum. Such situation is determined by wide scattering of experimental data; therefore, the chosen imaging method via component 1 (the dominant component that has 85% of the signal power) enables

Preprints (www.preprints.org) | NOT PEER-REVIEWED | Posted: 2 October 2019 doi:10.20944/preprints201910.0018.v1

Peer-reviewed version available at Forests 2019, 10, 959; doi:10.3390/f10110959

grouping of data. Figure 5 shows the fluorescence spectrum of PCA component 1 for different groups of experimental variants.

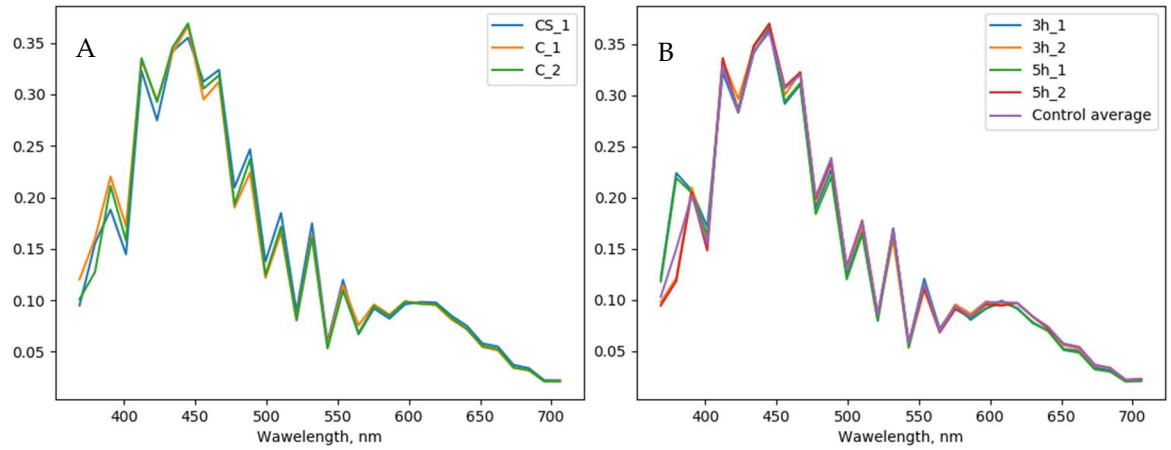

Figure 5. Component 1 of the pollen fluorescence amplitude, obtained by PCA method: A – control group; B – group of ozone-exposed pollen and control average

The results given in Figure 5 show similar pollen fluorescence spectrum of PCA component 1. This corresponds to the cases where pollen was not affected by ozone (the control group) but was stored in different conditions until the start of the experiment 1 or 5 months. Minor differences can be seen only in the wavelength range up to 500 nm of *Alnus glutinosa* pollen fluorescence amplitude. For this reason, analysing fluorescence peculiarities of ozone-exposed pollen, the mean of control group results was used. The fluorescence amplitude of PCA component 1 of pollen exposed to ozone is most pronounced at wavelengths up to 400 nm. The tendency is observed that there are minor differences between experimental groups that substantially differ with regard to time from pollen collection until the start of the experiment. Pollen that was stored for 5 months until the start of the experiment has the fluorescence spectrum of PCA component 1, which more resembles the one of the control group rather than of the experimental variant group whose pollen was kept at room temperature for 1 month. The results of PCA component 1 show that the duration of exposure to ozone in principal does not change the pollen fluorescence amplitude, which is important for calibration of real-time pollen detectors.

Summarising research results, it can be seen that essentially, the results of the principal PCA component in both control group and ozone-exposed pollen group do not differ (Figure 5). Conducting further analysis, dispersion charts of PCA component 1 and component 2 are given.

Assessing how changes in ozone-exposed pollen fluorescence are identified by real-time particle detector, we distinguished 4 main groups of results, which are presented in Fig. 6. In cases when pollen was briefly stored in room conditions and was not affected by ozone before the start of the experiment (control C_1), PCA component coefficients do not depend on each other, as shown in Fig. 6., A and C. These graphs demonstrate that changes occur in cases when pollen is exposed to ozone. In cases of both 3-hour exposure and 5-hour exposure, direct dependence with regard to PCA component coefficients emerges. Dependence of coefficients shows that the dominant light wavelength of fluorescence of the part of pollen is decreasing. The dependence straight of C_2 coefficients is insignificantly different compared to that of C_1. The obtained results may be determined by pollen maturation, because in the case of the second control, experiments were carried out 5 months after pollen dispersal from *Alnus glutinosa* catkins, which is 4 months later than time of C_1 experiment. It should be noted that fluorescence PCA component coefficients of ozone-exposed pollen in the experiment performed after 5 months in principal do not differ from the control (Fig. 6, B, D). The same trend is observed in the results of experiments when pollen was exposed to ozone for 3 hours and 5 hours. The assumption is formed that not only ozone can affect pollen fluorescence – storage conditions and duration of pollen shed from catkins can also become a modifying environmental factor determining variation in fluorescence properties.

Preprints (www.preprints.org) | NOT PEER-REVIEWED | Posted: 2 October 2019 doi:10.20944/preprints201910.0018.v1

Peer-reviewed version available at Forests 2019, 10, 959; doi:10.3390/f10110959

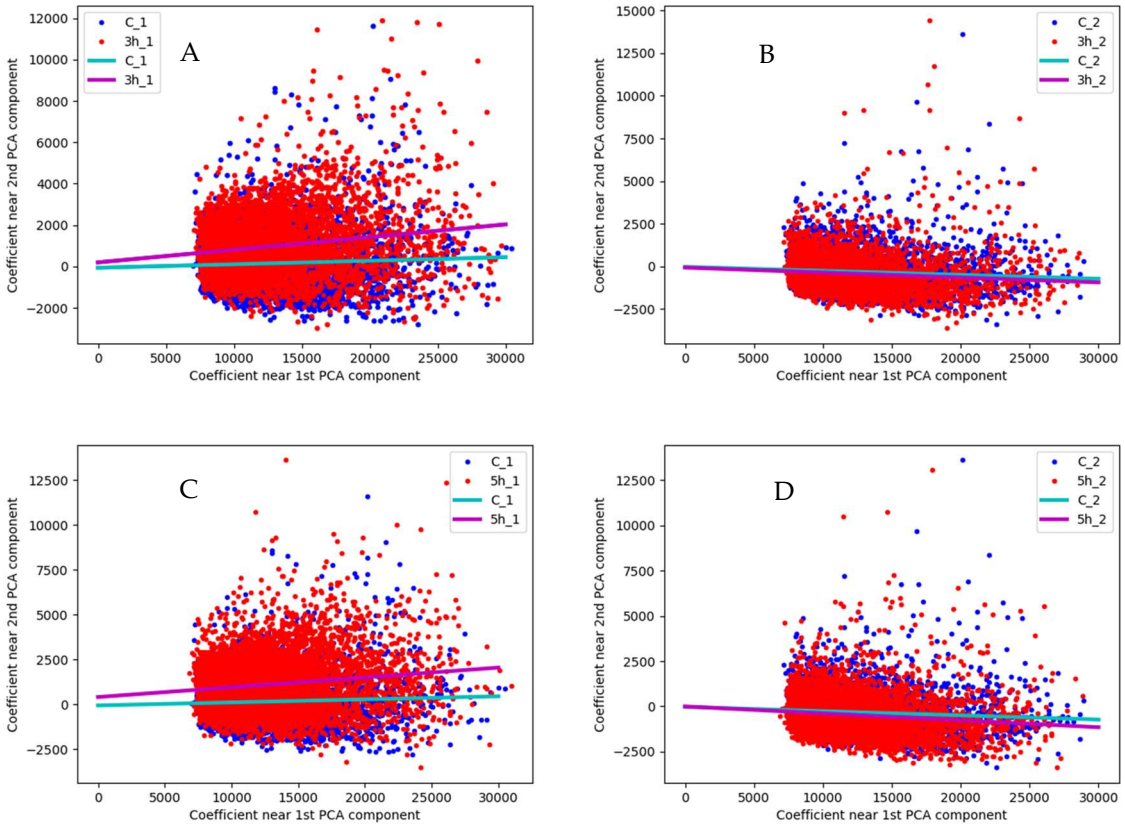

Figure 6. Dispersion charts of PCA components of experimental variant groups: A – 3-hour ozone exposure in comparison to control (pollen were stored for 1 month before the start of the experiment); B – 3-hour ozone exposure in comparison to control (pollen was stored for 5 months before the start of the experiment); C – 5-hour ozone exposure in comparison to control (pollen was stored for 1 month before the start of the experiment); D – 5-hour ozone exposure in comparison to control (pollen was stored for 5 months before the start of the experiment).

4. Discussion

This article analyses possibilities of identifying *Alnus glutinosa* pollen fluorescence peculiarities using manual (fluorescence microscopy) and automatic real-time devices. At present, there is an increasingly active search for tools and techniques enabling to replace the microscopic identification of pollen in routine aerobiological monitoring with recognition by automatic real time detectors. Operation of the latter is inseparable from fluorescence measurements of identified particles, which has been performed by spectrometers or fluorescence microscopes for many years. Various experiences have been performed analysing fluorescence properties of different types of pollen with tools enabling measurement of fluorescence peculiarities of particles and gathering plentiful valuable knowledge [7–9,30–31,36]. Often, available knowledge of fluorescence is difficult to apply in real-time measurements due to the different methods used so far (photo/electro-luminescence system with xenon lamps, various types of light-source-based fluorescence images etc.) [8,31,36] or measurement possibilities, using automatic real-time devices (deep-UV laser, etc.) [10–11,18]. On the other hand, there is a lack of studies analysing pollen fluorescence characteristics of a particular plant species in various aspects and searching for responses whether fluorescence peculiarities in a species can be modified or altered by environmental factors affecting pollen, e.g., air pollution [30,35], atmospheric condition [20,22,32], etc.

In this study, we used pollen that we collected from local *Alnus glutinosa* plants in the forest and did not process them anyhow additionally. We had a pure pollen fraction for control. Accurately selected samples enabled to obtain results that confirmed the fluorescence properties of pollen changed over time. An obvious example is disappearance of linear dependence of PCA component

coefficients in the case of ozone-exposed pollen fluorescence, when samples were stored for a longer time. This result indicates that assessing pollen samples of different origin and preparation, qualitative parameters of pollen samples must be taken into account as well.

We exposed *Alnus glutinosa* pollen to 5.83 ppm ozone to alter fluorescence properties of pollen and analysed digital images obtained under the fluorescence microscope and pollen data captured by automatic detector. Ozone is such substance that changes the composition of the cell wall [31], increases the content of allergen in pollen [35], decreases viability [37], and otherwise modifies pollen development. Most researchers [30,31] who use fluorescence-based methods to assess ozone exposure note that fluorescence of pollen exposed to ozone is changing. Our research verifies this fact by colour changes that can be noticed in the images of ozone-exposed *Alnus glutinosa* pollen, taken under the fluorescence microscope. Blue hues appearing next to dominant green colour can be seen. The visually noticed change is also confirmed by the analysis of digital images of pollen, obtained under the fluorescence microscope. It shows that the results of pollen stored in the ozone environment are shifting towards the blue portion of the spectrum.

The use of Rapid-E automatic particle detector, which identifies pollen by the fluorescence spectrum, in the study enabled to ascertain that ozone affects the pollen fluorescence spectrum. Data analysis supplemented the results obtained under a fluorescence microscope. Rapid-E shows dominance of blue colour in *Alnus glutinosa* pollen fluorescence spectrum. Analysing pollen fluorescence spectral feature, we obtained that the sharp peak of PCA 1 fluorescence amplitude of pollen not affected by ozone and ozone exposed pollen was identical, i.e., was at 450 nm. Meanwhile, the study of pure alder pollen, conducted by using a custom-build spectrometer, showed a sharp peak of *Alnus glutinosa* fluorescence at 420 nm [8]. Roshchina and Melnikova [30], who investigated changes in pollen fluorescence properties of other plant species due to ozone impact, found that fluorescence peaks of ozone-affected pollen had changed; e.g., control of *Philadelphus grandiflorus* (the variant that was not affected by ozone) had its peak at 465 nm, while having exposed to 5 ppm ozone, the peak shifted towards 475-480 nm. The authors confirm that in pollen whose fluorescence peak position was at blue or light blue colour, ozone treatment did not produce new peaks. In our experiments, there was no peak shift of fluorescence amplitude between ozone-exposed pollen and pollen not affected by ozone.

It should be noted that Rapid-E device registers the fluorescence spectrum as pollen is falling into device. The fluorescence induced laser is pulsed and emits the light beam as the pollen is approaching. Therefore, the moment of light beam activation is important for successful illumination of the pollen. In addition, the pollen itself is heterogeneous. Different locations can emit light of different wavelengths. It is therefore also important at what angle the pollen intersects with the exciting laser beam.

5. Conclusions

Digital images of ozone-exposed pollen observed under the fluorescence microscope showed the change of dominant green colour towards the blue spectrum. Meanwhile, the automatic device detects more pollen whose fluorescence in at the blue light spectrum. It should be noted that evaluating pollen fluorescence several months after exposure to ozone, no effect of ozone on fluorescence remains.

Summarizing the obtained results, it can be stated that both fluorescence-based devices employed in the study generate similar results-generating data. Data collection by the fluorescence microscope takes significantly longer and during the same time less data is accumulated than by automatic detector. However, both types of technologies can be useful for the analysis of pollen fluorescence characteristics.

Author Contributions: all the authors made significant contributions to this study. The conceptualization was performed by I. Š. and L. Š.; ozone generator created by A. L., microscopy by I. Š., L. Š., I. K., V. G, I. G.; experiments with particle detector were conducted by G. V., software and validation G. D. All authors contributed to the methodology, the interpretation of the results and the editing of the paper.

Funding: This research has been supported by the European Social Fund (project no. 09.3.3-LMT-K-712-01-0066) under grant agreement with the Research Council of Lithuania (LMTLT).

Acknowledgments: Authors thank the Lithuanian Hydrometeorological Service for meteorological data.

Conflicts of Interest: The authors declare no conflict of interest.

References

1. Boucher, A.; Hidalgo, P. J.; Thonnat, M.; Belmonte, J.; Galan, C.; Bonton, P.; Tomczak, R. Development of a semi-automatic system for pollen recognition. *Aerobiologia* **2002**, 18, 195–201.
2. Mitsumoto, K.; Yabusaki, K.; Kobayashi, K.; Aoyagi, H. Development of a novel real-time pollen-sorting counter using species-specific pollen autofluorescence. *Aerobiologia* **2010**, 26, 99–111.
3. Kiselev, D.; Bonacina, L.; Wolf, J. P. Individual bioaerosol particle discrimination by multi-photon excited fluorescence. *Opt Express* **2011**, 19, 24516–24521.
4. Asbeck, F. Fluoreszierender Blütenstaub. *Naturwissenschaften* **1955**, 42, 632.
5. Van Gijzel, P. Autofluorescence of fossil pollen and spores with special reference to age determination and coalification. *Leidse Geologische Mededelingen* **1967**, 40, 261–317.
6. Sivaguru, M.; Urban, M.A.; Fried, G.; Wesseln, C.J.; Mander, L.; Punyasena, S.W. Comparative performance of airyscan and structured illumination superresolution microscopy in the study of the surface texture and 3D shape of pollen. *Microsc. Res. Tech.* **2018**, 81, 101–114.
7. Ronneberger, O.; Schultz, E.; Burkhardt, H. Automated pollen recognition using 3D volume images from fluorescence microscopy. *Aerobiologia* **2002**, 18, 107–115.
8. O'Connor, D.J.; Iacopino, D.; Healy, D.A.; O'Sullivan, D.; Sodeau, J.R. The intrinsic fluorescence spectra of selected pollen and fungal spores. *Atmos Environ X* **2011**, 45, 6451–6458.
9. Stanley, W.R.; Kaye, P.H.; Foot, V.E.; Barrington, S.J.; Gallagher, M.; Gabey, A. Continuous bioaerosol monitoring in a tropical environment using a UV fluorescence particle spectrometer. *Atmos Sci Lett* **2011**, 12, 195–199.
10. Crouzy, B.; Stella, M.; Konzelmann, T.; Calpini, B.; Clot, B. All-optical automatic pollen identification: towards an operational system. *Atmos. Environ.* **2016**, 140, 202–212.
11. Šaulienė, I.; Šukienė, L.; Daunys, G.; Valiulis, G.; Vaitkevičius, L.; Matavulj, P.; Brdar, S.; Panic, M.; Sikoparija, B; Clot, B.; Crouzy, B.; Sofiev, M. Automatic pollen recognition with the rapid-E particle counter: The first-level procedure, experience and next steps. *Atmos. Meas. Tech.* **2019**, 2, 1–33.
12. Buters, J.T.M.; Antunes, C.; Galveias, A.; Bergmann, K.C.; Thibaudon, M.; Galán, C.; Schmidt-Weber C.; Oteros, J. Pollen and spore monitoring in the world. *CLIN TRANSL ALLERGY* **2018**, 8, 9.
13. Hirst, J.M. An automatic volumetric spore trap. *Ann Appl Biol* **1952**, 39, 257–265.
14. Galán, C.; Smith, M.; Thibaudon, M.; Frenguelli, G.; Oteros, J.; Gehrig, R.; Berger, U.; Clot, B., Brandao, R.; EAS QC working group. Pollen monitoring: minimum requirements and reproducibility of analysis. *Aerobiologia* **2014**, 30, 385–395.
15. Gottardini, E.; Rossi, S.; Cristofolini, F.; Benedetti, L. Use of Fourier transform infrared (FT-IR) spectroscopy as a tool for pollen identification. *Aerobiologia* **2007**, 23, 211–219.
16. Mitsumoto, K.; Yabusaki, K.; Aoyagi, H. Classification of pollen species using autofluorescence image analysis. *J. Biosci. Bioeng.* **2009**, 107, 90–94.
17. Oteros, J.; Pusch, G.; Weichenmeier, I.; Heimann, U.; Möller, R.; Röseler, S.; Traidl-Hoffmann, C.; Schmidt-Weber, C.; Buters, J.T. Automatic and online pollen monitoring. *Int. Arch. Allergy Immunol.* **2015,** 167, 158–166.
18. Sofiev, M. On possibilities of assimilation of near-real-time pollen data by atmospheric composition models. *Aerobiologia* **2019**, 35, 523–531.
19. Kasprzyk, I. Comparative study of seasonal and intradiurnal variation of airborne herbaceous pollen in urban and rural areas. *Aerobiologia* **2006**, 22, 185–195.
20. Tormo Molina, R.; Silva Palacios, I.; Muñoz RodrÍguez, A.F.; Tavira Muñoz, J.; Moreno Corchero, A. Environmental factors affecting airborne pollen concentration in anemophilous species of Plantago. *Ann. Bot.* **2001**, 87, 1–8.
21. García-Mozo, H.; Oteros, J.A.; Galán, C. Impact of land cover changes and climate on the main airborne pollen types in Southern Spain. *Sci. Total Environ.* **2016**, 548, 221–228.

22. Lebourgeois, F.; Delpierre, N.; Dufrêne, E.; Cecchini, S.; Macé, S.; Croisé, L.; Nicolas, M. Assessing the roles of temperature, carbon inputs and airborne pollen as drivers of fructification in European temperate deciduous forests. *Eur J For Res* **2018**, 137, 349–365.
23. Sofiev, M.; Siljamo, P.; Ranta, H.; Rantio-Lehtimäki, A. Towards numerical forecasting of long-range air transport of birch pollen: theoretical considerations and a feasibility study. *Int J Biometeorol* **2006**, 50, 392–402.
24. Skjøth, C.A.; Sommer, J.; Stach, A.; Smith, M.; Brandt, J. The long-range transport of birch (Betula) pollen from Poland and Germany causes significant pre-season concentrations in Denmark. *Clin. Exp. Allergy* **2007**, 37, 1204–1212.
25. Siljamo, P.; Sofiev, M.; Ranta, H. An approach to simulation of long-range atmospheric transport of natural allergens: an example of birch pollen. In *Air pollution modeling and its application XVII*, Publisher: Springer, Boston, MA, 2007; pp. 331-339.
26. Smith, M.; Skjøth, C.A.; Myszkowska, D.; Uruska, A.; Puc, M.; Stach, A.; Balwierz, Z.; Chlopek K.; Piotrowska, K.; Kasprzyk I.; Brandt, J. Long-range transport of Ambrosia pollen to Poland. *Agric For Meteorol* **2008**, 148, 1402–1411.
27. Veriankaitė, L.; Siljamo, P.; Sofiev, M.; Šaulienė, I.; Kukkonen, J. Modelling analysis of source regions of long-range transported birch pollen that influences allergenic seasons in Lithuania. *Aerobiologia* **2010**, 26, 47–62.
28. de Weger, L.A.; Pashley, C.H.; Šikoparija, B.; Skjøth, C.A.; Kasprzyk, I.; Grewling, Ł.; Thibaudon, M.; Magyar, D.; Smith, M. The long distance transport of airborne Ambrosia pollen to the UK and the Netherlands from Central and south Europe. *Int J Biometeorol* **2016**, 60, 1829–1839.
29. Sofiev, M. On impact of transport conditions on variability of the seasonal pollen index. *Aerobiologia* **2017**, 33, 167–179.
30. Roshchina, V.V.; Mel'nikova, E.V. Pollen chemosensitivity to ozone and peroxides. *Russ. J. Plant Physiol.* **2001**, 48, 74–83.
31. Roshchina, V.V.; Yashin, V.A.; Kuchin, A.V. Fluorescent analysis for bioindication of ozone on unicellular models. *J Fluoresc* **2015**, 25, 595–601.
32. Albertine, J.M.; Manning, W.J.; DaCosta, M.; Stinson, K.A.; Muilenberg, M.L.; Rogers, Ch.A. Projected carbon dioxide to increase grass pollen and allergen exposure despite higher ozone levels. *PLoS One* **2014**, 9, e111712.
33. Beck, I.; Jochner, S.; Gilles, S.; McIntyre, M.; Buters, J.T.; Schmidt-Weber, C.; Behrendt, H.; Ring, J.; Menzel, A.; Traidl-Hoffmann, C. High environmental ozone levels lead to enhanced allergenicity of birch pollen. *PLoS One* **2013**, 8, e80147.
34. Kanter, U.; Heller, W.; Durner, J.; Winkler, J.B.; Engel, M.; Behrendt, H.; Pfeifer M.; Mayer, K. Molecular and immunological characterization of ragweed (Ambrosia artemisiifolia L.) pollen after exposure of the plants to elevated ozone over a whole growing season. *PLoS One* **2013**, 8, e61518.
35. Frank, U.; Ernst, D. Effects of NO2 and ozone on pollen allergenicity. *Front Plant Sci* **2016**, 7, 91.
36. Gottardini, E.; Cristofolini, F.; Paoletti, E.; Lazzeri, P.; Pepponi, G. Pollen viability for air pollution bio-monitoring. *J Atmos Chem* **2004**, 49, 149–159.
37. Pasqualini, S.; Tedeschini, E.; Frenguelli, G.; Wopfner, N.; Ferreira, F.; D'Amato, G.; Ederli, L. Ozone affects pollen viability and NAD (P) H oxidase release from Ambrosia artemisiifolia pollen. *Environmental Pollution* **2011**. 159, 2823–2830.
38. Zhu, C.; Farah, J.; Choël, M.; Gosselin, S.; Baroudi, M.; Petitprez, D.; Visez, N. Uptake of ozone and modification of lipids in Betula Pendula pollen. *Environmental Pollution* **2018**, 242, 880–886.
39. Ministry of Environment. Lithuania's forests. Available online: http://www.amvmt.lt/index.php/nacionaline-misku-inventorizacija2/leidiniai/lietuvos-miskai (accessed on 06-09-2019).
40. Šaulienė, I.; Šukienė, L.; Kainov, D.; Greičiuvienė, J. The impact of pollen load on quality of life: a questionnaire-based study in Lithuania. *Aerobiologia* **2016**, 32, 157–170.
41. Mäkinen, Y.; Rantio-Lehtimaki, A. Diurnal variation of airborne fungal spores in Turku, Finland, in 1974. *Rep. Aerobiol. Lab. Univ. Turku* **1979**, 1, 1–27.
42. Jochner-Oette, S.; Simmons, M.; Jetschni, J.; Menzel, A. Impacts of land clearance by fire on spatial variation of mountain cedar pollen concentrations in Texas. *Landsc Urban Plan* **2017**, 162, 178–186.
43. Sulmont, G. (Ed.). *The pollen content of the air: identification key*. Studios Bouquet, France, 2011.